

## Natural intrinsic *EX* center in thermal SiO<sub>2</sub> on Si: <sup>17</sup>O hyperfine interaction

A. Stesmans and F. Scheerlinck

*Department of Physics, Katholieke Universiteit Leuven, 3001 Leuven, Belgium*

(Received 6 December 1993; revised manuscript received 15 April 1994)

The atomic structure of the intrinsic *EX* defect naturally generated in thermal SiO<sub>2</sub> on Si has been analyzed by electron spin resonance on 51% <sup>17</sup>O enriched (111)Si/SiO<sub>2</sub> structures. Although the hyperfine structure could be only partly observed, the results indicate that the *EX* center is an excess-oxygen defect, the defect core incorporating several O atoms which appear not to be entirely equivalent sites with regard to hyperfine interaction. The emanating working model is a Si vacancy in SiO<sub>2</sub>, where an unpaired electron is delocalized over the four bordering O atoms, resulting in an effectively pure *s* state, which is subject to <sup>29</sup>Si superhyperfine interaction with neighboring Si sites.

### I. INTRODUCTION

The characterization of defects in Si/SiO<sub>2</sub> has become an intensive research item ever since this structure became an indispensable unit in semiconductor devices. In the list of possible intrinsic (i.e., not impurity related) defects, one may discriminate between *natural* defects, generated during the thermal Si/SiO<sub>2</sub> growth process, and *damage* defects, introduced in a postoxidation stage by irradiation with some kind of energetic species (e.g.,  $\gamma$  and *x* photons, electrons, ions). An archetype of the latter is the intensively studied *E'* defect in SiO<sub>2</sub>. Various species have been distinguished by electron-spin resonance (ESR), the most common entity of all being elucidated as a defect Si hybrid orbital at the site of an O vacancy—denoted as O<sub>3</sub>≡Si.<sup>1</sup> ESR has proven to be an indispensable tool when it comes to structural identification of such defects: The symmetry of the defect wave function is reflected in the measured *g* diadic and—most vital in view of structure determination—the hyperfine (hf) structure (originating from <sup>29</sup>Si and <sup>17</sup>O nuclei in *a*-SiO<sub>2</sub>) carries information about the exact atomic surrounding of the unpaired defect spin.

Perhaps of even more fundamental and practical importance are *natural* intrinsic defects, where in the thermal Si/SiO<sub>2</sub> entity there so far seems to exist only one class; that is, the mismatch-induced interface defects, the so-called *P<sub>b</sub>* defects when ESR active. It is a major achievement of ESR, in combination with theoretical analysis, to have identified and characterized these *P<sub>b</sub>* defects at the Si/SiO<sub>2</sub> interface in astounding detail.<sup>2–8</sup>

Interestingly, an ESR observation of an additional natural defect, in as-grown thermal SiO<sub>2</sub> on (111)Si denoted as the *EX* center, has recently been added to the latter class.<sup>9,10</sup> The center displays a remarkably isotropic three-peak ESR spectrum: it exhibits a narrow Voigt-shape-like central peak, at  $g = 2.00246 \pm 0.00003$ , amid a hf doublet of 16.1-G splitting, with the doublet lines slightly broader than the central line, i.e., peak-to-peak widths  $\Delta B_{pp} \approx 1.1$  and 1.2 G for the central line and hf peaks, respectively. No hf lines other than the 16.1-G doublet were observed, although a 1000-G window cen-

tered at the *EX* central line was thoroughly scanned using signal averaging. In subsequent work the center's growth aspects [identical for (111) and (001)Si/SiO<sub>2</sub>] in the oxidation temperature range  $T_{ox} \approx 700$ – $930$  °C were extensively investigated,<sup>11</sup> with two major findings: first, the areal density of ESR-active defects ( $N_A^{EX}$ ) is determined solely by the grown oxide thickness ( $d_{ox}$ ), a maximum occurring for  $d_{ox} \approx 125$  Å; second, the defects reside in the top  $\sim 40$  Å of the SiO<sub>2</sub> films, distributed approximately along a hemi-Gaussian density-depth profile centered at the ambient/SiO<sub>2</sub> interface. An important general conclusion of these studies was the *intrinsic* nature of the *EX* defect, that is, not directly related to impurity incorporation in the Si oxide in the sense that no impurity makes up the core of the defect.

As studied in isotopically unenriched thermal SiO<sub>2</sub>, this culminated in a working model for the atomic structure of the ESR-active *EX* center,<sup>9</sup> picturing it as an intrinsic hole defect in SiO<sub>2</sub>, where the unpaired spin is delocalized over sufficient tetrahedral orbitals to result in an effectively pure *s* state. The resolved hf structure indicates that this electron is not primarily localized on a Si site, though it is involved in <sup>29</sup>Si hf interaction with three or four equivalent neighboring Si sites. This is about as far as the provisional model, as derived from detailed ESR study on isotopically unenriched Si/SiO<sub>2</sub> samples, could go. Evidently then, the next step on the route to atomic identification implies isotopic enrichment, which technique, in combination with ESR, has emerged as the unequalled structural identification tool. One such step, i.e., the study of  $\sim 51\%$  <sup>17</sup>O enriched (111)Si/SiO<sub>2</sub> entities, is addressed here. With an <sup>17</sup>O natural abundance of only 0.037%, it is obvious that no O hf interaction could possibly be detected in previous work. Hence, with this <sup>17</sup>O enrichment the eventual O involvement in the defect's core structure is examined.

### II. EXPERIMENTAL DETAILS

Two isotopically enriched Si/SiO<sub>2</sub> samples, labeled A1 and B1, were grown on HF-precleaned *p*-type (111)Si slices at 800 °C in  $\sim 24$ -kPa dry O<sub>2</sub> enriched to 51.22%

<sup>17</sup>O. Samples A1 and B1 were grown for  $t_{\text{ox}}=358$  and 255 min, respectively, and subsequently exhaustively degassed at 790 °C for about 1 h to maximize  $N_A^{EX}$ .<sup>11</sup> For comparative purposes, (111)Si/SiO<sub>2</sub> samples (A2 and B2) were also grown in unenriched O<sub>2</sub> under otherwise *identical* oxidation conditions.

ESR experiments were carried out at 4.3 K in a K-band ( $\approx 20.2$  GHz) spectrometer in derivative absorption mode (see Ref. 12 for more experimental details). Areal spin densities were determined relative to a Si:P marker sample of known number of spins<sup>13</sup> through double numerical integration of the respective derivative absorption signals  $dP_{\mu a}/dB$ , where  $P_{\mu a}$  and  $B$  are the absorbed microwave power and the magnitude of the magnetic induction, respectively.

### III. EXPERIMENTAL RESULTS

Typical EX ESR spectra, measured at 4.3 K on samples A1 and A2, with **B** parallel to the (111) interface,<sup>14</sup> are shown in Fig. 1. The signals labeled  $EX_c$  and Si:P stem from the EX defect and the Si:P reference sample ( $g=1.998\,69\pm 0.000\,02$ ), respectively. The spectra in Fig. 1 bear out, in a concise way, the drastic effect of the  $\sim 51\%$  <sup>17</sup>O enrichment: the weak  $EX_c$  signal in Fig. 1(b) is the remnant of the strong central signal of the unenriched EX spectrum in Fig. 1(a). The intensity of the

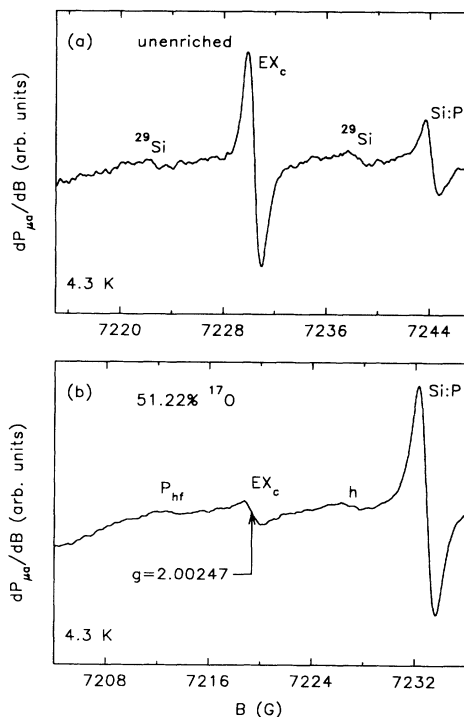


FIG. 1. K-band first-derivative absorption spectra of the EX center, measured at 4.3 K with **B** parallel to the (111) interface (a) before (sample A2) and (b) after (sample A1) isotopic enrichment to 51.22% <sup>17</sup>O, demonstrating the dramatic impact on the central EX line ( $EX_c$ ). Si:P denotes the Si:P reference signal [at  $g(4.3\text{ K})=1.998\,69$ ], while  $^{29}\text{Si}$  and  $h$  denote the  $^{29}\text{Si}$  hf lines of the EX center in the unenriched sample, and part of the EX <sup>17</sup>O hf structure in the enriched sample, respectively.

remaining central EX line is  $(3.7\pm 0.4)\times 10^{10}\text{ cm}^{-2}$ , which only amounts to  $\sim 9.3\%$  of the full EX intensity of sample A2. So, assuming that equal EX densities have been grown in the <sup>17</sup>O unenriched (A2) and enriched (A1) samples, there is a reduction of  $\sim 90\%$  in the central signal intensity due to 51% <sup>17</sup>O enrichment. It is further observed that the central EX resonance is broadened from  $\sim 1$  G (sample A2) to about 1.5 G, an effect which is likely due to hf interaction with remote <sup>17</sup>O nuclei.

The downward slope at the low-field side of Fig. 1(b) is part of the strong  $P_b$  signal, while some <sup>31</sup>P hf structure also seems to be present: variation of the microwave power allowed us to identify the resonance labeled  $P_{hf}$  as the low-field part of the <sup>31</sup>P hf doublet (splitting  $a=42.0$  G) (Ref. 15) originating from uncompensated P states formed during thermal oxidation in the near interfacial Si layers—a common result of the P pileup effect.<sup>16</sup> The line labeled  $h$ ,  $\sim 7.5$  G away from the central EX line, was observed to be a reproducible part of the EX spectrum: when gradually increasing the incident microwave power above  $-60$  dBm, it was found to saturate much like the central EX line. It is interpreted as part of the <sup>17</sup>O hf structure. On the low-field side of  $EX_c$ , unfortunately, the broad  $P_b$  resonance tail and the P hf obscure possible hf structure, and, hence, also the presumed 7.5-G symmetric counterpart of line  $h$ .

No additional reproducible <sup>17</sup>O hf structure could be discerned, although in terms of relative intensities there must be additional <sup>17</sup>O hf structure in the <sup>17</sup>O-enriched case.

To gain more information about the EX <sup>17</sup>O hf structure outside the central line, this clearly dictates a significant enhancement of the signal-to-noise (S/N) ratio. Different approaches were tried: Like most defects in *a*-SiO<sub>2</sub>, the EX center is very sensitive to microwave saturation. So, by introduction of He atoms in the SiO<sub>2</sub> network (postdehydrogenation anneal in He at 300 °C for 11 min), we tried positively to modify the saturation behavior of the EX signal,<sup>17</sup> though without success. Neither did ESR measurements at  $T > 4.3$  K (with an expected reduction in saturability) lead to much improvement.

Next the effective sample area in the cavity was optimized by stacking more Si/SiO<sub>2</sub> slices (measuring  $2\times 9$  mm<sup>2</sup>) realized through Si substrate thinning in an isotropic etch. Thinning down to  $\sim 25$   $\mu\text{m}$  resulted in an increase of sample area from  $\sim 5$  cm<sup>2</sup> (sample A1) to about 22.5 cm<sup>2</sup> (sample B1) resulting in a significant increase in the S/N ratio. An overview spectrum, recorded on sample B1 at 4.3 K without the Si:P reference sample, is presented in Fig. 2. Beside the central EX line ( $EX_c$ ), a huge  $P_b$  signal is present ( $\Delta B_{pp}\approx 7$  G for B1 [111]). Part of the EX <sup>17</sup>O hf structure has now become more evident: the presence of the 7.5-G line ( $h$ ) is clearly visible while the structure labeled  $h'$  about 22 G remote from the central EX line could reproducibly be observed, and is also ascribed to <sup>17</sup>O hf structure. This assignment is consistent with a hf splitting  $a\approx 15$  G, but in terms of <sup>17</sup>O (nuclear spin  $I=\frac{5}{2}$ ) hf interactions it must be admitted that the remaining hf structure then remains unresolved (*vide infra*). The unequal saturation behavior allowed us

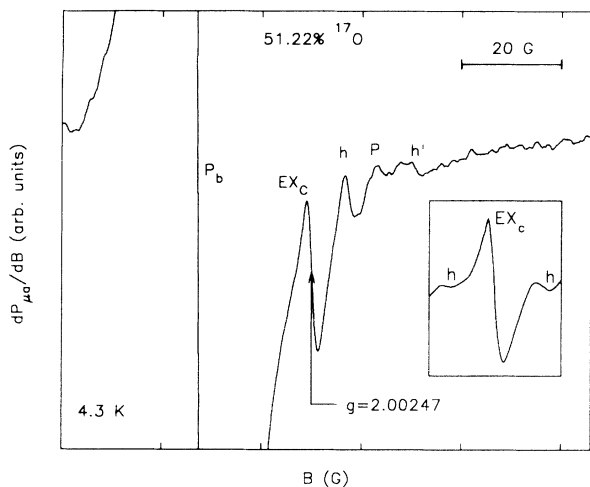


FIG. 2. Broad-scan first-derivative absorption ESR spectrum, measured at 4.3 K on sample B1 for  $\mathbf{B} \parallel (111)$ , without Si:P marker sample.  $EX_c$ ,  $P_b$ , and  $P$ , respectively, denote the central  $EX$  resonance, the  $P_b$  signal, and a signal due to  $P$  pileup; the lines  $h$  and  $h'$  are interpreted as part of the  $EX$   $^{17}\text{O}$  hf structure. In the inset, the  $P_b$  background has been subtracted, clearly revealing the  $\sim 15$ -G  $h$  doublet, ascribed to  $^{17}\text{O}$  hf structure.

to identify the signal labeled  $P$  in Fig. 2 as the “central pair”  $P$  signal ( $g = 1.99858$ ) (Ref. 16) introduced during thermal oxidation by the  $P$  pileup effect. The unavoidably copresent, large  $P_b$  signal masks the low-field hf structure of the  $EX$  center. However, background subtraction did reveal the counterpart of the 7.5-G line, as shown in the inset to Fig. 2. The areal density of the central  $EX$  line amounts to  $(5.5 \pm 0.5) \times 10^{10} \text{ cm}^{-2}$  which, compared with sample B2, is equivalent to  $\sim 9.7\%$  of the full unenriched  $EX$  signal (no  $^{17}\text{O}$ ), in agreement with the A-sample data.

Though one might have liked to resolve more structure, this apparently is as far as present ESR analysis can reasonably go. Detection of the full  $^{17}\text{O}$  hf structure will require a *drastic* step in signal enhancement that is, e.g., not just an increase of the effective sample area, but, in one way or another, creation of much larger  $EX$  densities or by making the  $EX$  bath more “saturation hard.” At present, however, an understanding of the  $EX$  growth mechanism(s) is still lacking.<sup>11</sup> However, part of the  $^{17}\text{O}$  hf structure is resolved, from which useful information can be extracted.

#### IV. INTERPRETATION AND DISCUSSION

##### A. An O-centric defect

A major experimental conclusion is that  $\sim 51\%$   $^{17}\text{O}$  enrichment leads to a reduction of  $\sim 90\%$  in central signal intensity. As this inference will serve as the basis for all further interpretation, we should emphasize that it bears totally on the reproducibility of  $EX$  concentrations among samples grown under identical conditions. This assumption, however, appears fully validated by previous extended work. The profound impact then effectuated by

$^{17}\text{O}$  enrichment leads to three important conclusions. First, the  $EX$  center is an O-centric defect, with the unpaired electron mainly localized on O core sites. It explains how the major part ( $\sim 90\%$ ) of the prominent  $EX$  central signal is “lost” as a result of strong unpaired electron– $^{17}\text{O}$  hf interactions resulting in excessively split hf multiplets ( $^{17}\text{O}$  has  $I = \frac{5}{2}$ ): Simplified linear combination of atomic orbitals (LCAO) calculations indicate that a pure  $2s$   $^{17}\text{O}$  orbital would give rise to an atomic hf splitting<sup>1</sup>

$$a_{\text{atomic}} = \frac{2}{3} \mu_0 g_N \mu_N |\psi_{2s}(0)|^2 \approx 1660 \text{ G}, \quad (1)$$

where  $g_N \mu_N I$  is the  $^{17}\text{O}$  nuclear magnetic moment and  $|\psi_{2s}(0)|^2$  the density of the  $2s$  wave function at the  $^{17}\text{O}$  nucleus;  $\mu_0$ ,  $g_N$ , and  $\mu_n$  are the magnetic permeability of the vacuum, the nuclear  $g$  factor, and the nuclear magneton, respectively. Hence, even with only a very small admixture of  $s$  character into a  $2p$  nonbonding orbital, there can exist excessive hf splitting.<sup>18</sup> With the overall intensity then attained, these strongly split hf multiplet components are likely to become undetectable for two reasons. First, because of the multiplet component character, as interaction with a single  $^{17}\text{O}$  nucleus leads to a sextet. Second, because of the fact that the farther a hf component is split out, the more strongly it becomes broadened: this results from weak site-dependent modifications in the distribution of the unpaired electron’s wave function over the interacting nuclei due to the local weak alterations in the defect atomic structure when embedded in an amorphous (i.e.,  $a\text{-SiO}_2$ ) structure (the glass effect).<sup>19</sup> If, instead, the center’s core consists of a defect Si orbital, where the O atoms occupy first- or higher-order neighbor sites, one should merely expect a weak superhyperfine (shf) broadening of the central signal, probably  $\sim 1$  G; the signal intensity (the area under the absorption curve), however, remains unchanged. An estimate of the expected broadening in the latter case may be obtained from the measured  $^{17}\text{O}$  shf interaction of the  $E'$  center in glassy  $\text{SiO}_2$ .<sup>20</sup> There, the shf interaction of the unpaired spin in the  $sp^3$ -like Si orbital with the three (first-neighbor) basal O nuclei was measured, resulting in an average isotropic splitting  $a_{\text{shf}} \approx 0.8$  G (while no anisotropic shf component could be resolved).

The second conclusion is that, while  $EX$  concerns an O-centric defect, it *cannot be* a one-O core defect. In this case, one would expect to have  $\sim 49\%$  of the initial intensity left in the central peak after  $\sim 51\%$   $^{17}\text{O}$  enrichment, which is not what is observed. The much reduced ( $\sim 90\%$ ) central-peak intensity, in effect, strongly indicates that the unpaired electron is primarily *distributed* over various, possibly equivalent, O sites. The weak remaining central-line intensity reflects, with  $p(^{17}\text{O}) = 0.5122$ , just the small probability of finding none of the equivalent O core sites occupied by an  $^{17}\text{O}$  isotope in addition to some HF intensity which is “split back” into the central line. The sum of these two contributions can be as low as  $(1-p)^3 + 18(1-p)(p/6)^2 \approx 18.0\%$  and  $(1-p)^4 + 36(1-p)^2(p/6)^2 + 140(p/6)^4 \approx 12.6\%$ , for interaction with  $N=3$  and 4 equivalent O sites, respectively. This finding regarding the delocalized nature of the unpaired

spin complies with a previous conclusion drawn from the *EX* defect's remarkable *g*-matrix isotropy:<sup>9</sup> There it was concluded that such perfect *g* isotropy for a defect embedded in  $\alpha$ -SiO<sub>2</sub> strongly suggests that the unpaired electron is delocalized over various orbitals (atomic sites), so that an effectively pure *s* state is left as the *p* character of the defect wave function is spatially averaged out. This inference provides a first element of consistency.

Third, if assuming that part of the <sup>17</sup>O hf structure has been resolved, the line-shape symmetry—that is, the closely paramagnetic shape of the *A/B* ratio  $\approx 1$  (*A* and *B* representing the heights of the low- and high-field peaks, respectively)—of the observed hf signals then indicates that this hf interaction is largely isotropic,<sup>18</sup> with an observed splitting  $a \sim 14$  G: Should the hf tensor instead show significant anisotropy, one would expect the amorphous character of the SiO<sub>2</sub> environment to turn the hf signal into some kind of powder pattern,<sup>1</sup> the particular shape purely reflecting the *EX* defect's <sup>17</sup>O hf tensor symmetry and interaction strength, as no *g* anisotropy is present. In contrast, there is little experimental evidence for such a feature.

However, thinking along extreme lines, one could hope to refute this conclusion by recourse to a strongly anisotropic <sup>17</sup>O hf tensor. For instance, in terms of the simple, though not uncommon, case of axial symmetry, one could suppose a large difference between *A*<sub>∥</sub> and *A*<sub>⊥</sub>. This then, still reasoning in the absence of *g* anisotropy, would lead to a <sup>17</sup>O hf derivative spectrum in which each hf signal consists roughly of an upward (low field) and downward (high field) peak separated by  $\sim (A_{\parallel} - A_{\perp})$  G. One could thus presume that only one of these peaks—either the low- or high-field peak—of each <sup>17</sup>O hf component is resolved, as is observed, e.g., for the <sup>17</sup>O en-

riched nonbridging oxygen-associated hole center (NBOHC).<sup>18</sup> But, again, this is clearly not the case for the *EX* spectrum.

It may be instructive to compare the *EX* <sup>17</sup>O hf interaction with that observed for the well-identified NBOHC, generally denoted as  $\equiv\text{Si}-\text{O}^{\cdot}$ , in  $\gamma$ -irradiated high-OH fused silica [variably called the "wet" OHC (Ref. 18)]. There the value  $|a| \approx 26$  G (Ref. 21) has been deduced for the *2p* nonbonding orbital of the NBOHC, the isotropic part of the hf interaction arising from core-polarization effects in addition to a very small admixture ( $\sim 0.007\%$ ) of the *s* orbital into the *2p* orbital. Reasoning then, in an idealized way, that the unpaired spin should be evenly localized over four O sites, it seems reasonable to expect a reduction of  $|a|$  toward 6.5 G, somewhat smaller than the observation ( $\sim 14$  G). This tends to add some confidence to the postulated basic ingredients of the *EX* atomic structure, while again revealing some self-consistency: the magnitude of the observed <sup>17</sup>O hf interaction complies with the *delocalized* nature of the unpaired O orbital derived from other ESR features.

### B. Basic model

With the foregoing accomplished, and taking into account the *intrinsic* nature of the defect, one may feel tempted to propose the idealized working model for the *EX* defect depicted in Fig. 3(f). In broad terms, this model pictures the *EX* defect as a hole trapped at the site of a Si vacancy, where two O atoms are (weakly) pair bonded while the remaining unpaired electron is postulated to be delocalized over the bordering O atoms. (To stay fair, it needs to be remarked that, purely based on the ESR results, the modeling could equally well start from a

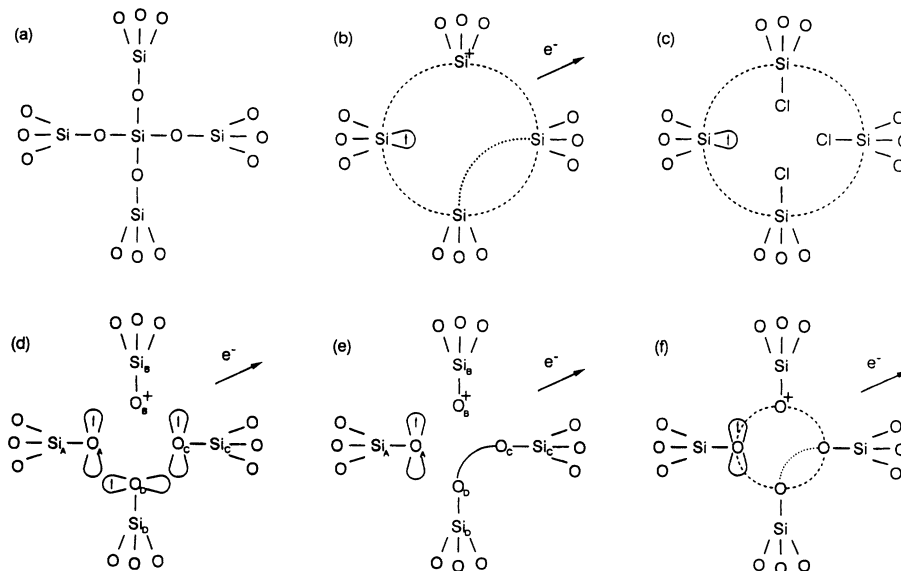


FIG. 3. Schematic pictures of clusters in  $\alpha$ -SiO<sub>2</sub> pertaining to the various defect models in the text: (a) perfectly stoichiometric SiO<sub>2</sub>, (b) a SiO<sub>4</sub> vacancy, (c) the Cl-dressed SiO<sub>4</sub> vacancy model suggested for the *E*<sub>s</sub> defect (Ref. 22), (d) the unrelaxed Si vacancy short of one electron, (e) one possible configuration of the positively charged Si vacancy in the dynamic Jahn-Teller picture, and (f) the *EX* defect pictured as a positively charged Si vacancy with an unpaired spin delocalized over four O atoms. In (a)–(f), a dashed circle emphasizes the delocalized nature of the unpaired spin, while a dotted bow represents dynamic (weak) bond formation and breaking.

trapped electron; *vide infra*.) When referring to the particular *EX* generation process, i.e., grown in during thermal oxidation at elevated temperatures ( $T_{\text{ox}} \approx 700\text{--}930^\circ\text{C}$ ), the delimiting  $\equiv\text{Si}\text{--O}$  fragments are likely to have reached a fully thermally relaxed state in compliance with minimum-energy constraints.

The *EX* model has much in common with that proposed for the  $E'_\delta$  defect, a radiation-induced defect observed by ESR in synthetic silicas. This center<sup>22</sup> was interpreted as the next species of the traditional  $E'$  defects—thus classifying it as a nonbonding Si  $sp^3$  orbital—then comprising the variants  $E'_\alpha$ ,  $E'_\beta$ , and  $E'_\gamma$ , in  $\alpha\text{-SiO}_2$ ,<sup>23</sup> based on the fact that it shared one principal  $g$  value (i.e.,  $g_1=2.0018$ ) with the  $E'$  family. However, particular changes in the  $^{29}\text{Si}$  hf structure in addition to the much reduced  $g$ -matrix anisotropy ( $g_1=2.0018$ ,  $g_2=g_3=2.0021$ ) as compared to the traditional  $E'$  defects, urged for adding a new concept to the modelling, i.e., *delocalization* of the unpaired spin over several Si atoms vis-à-vis the description of an unpaired electron in one nonbonding Si hybrid orbital, the basic entity for all  $E'$  variants so far identified. As shown in Fig. 3(c), the  $E'_\delta$  defect was pictured as a  $\text{SiO}_4$  vacancy in an otherwise continuous random network, dressed with three Cl atoms, with the unpaired spin delocalized over the four bordering Si atoms. In turn, this  $E'_\delta$  model for which the Cl dressing aspect has now been abandoned,<sup>24</sup> has much of its roots in the existence of the OH-decorated  $\text{SiO}_4$  vacancies in  $\alpha$  quartz.<sup>25</sup> It thus appears that from then on, the  $E'$  family is subdivided into two classes, namely traditional (localized)  $E'$  centers and delocalized  $E'$  defects.

With respect to the  $E'_\delta$  proposal, the *EX* defect model starts from a Si vacancy [Fig. 3(d)] rather than a  $\text{SiO}_4$  vacancy [Fig. 3 (b)], the unpaired electron now being delocalized over four oxygen—instead of Si—atoms bordering the cavity, where no additional dressing by a particular foreign atom is presumed. Staying within the common  $\text{SiO}_2$  defect terminology, another way to look at the *EX* model is as an assembly of four NBOHC entities arranged in a tetrahedral-centric way, short of one electron. Or, when weak O-O bonds are allowed to form, the scheme, in its neutral state, may be read as two oppositely arranged peroxy linkages.

This model, though perforce highly schematic, is a simple *least-complication* model believed to basically incorporate all physicochemical ingredients needed to account for the salient *EX* ESR properties, in particular those extracted from the present  $^{17}\text{O}$  enrichment data. These imply the following.

(1) The model in Fig. 3(f) pictures the *EX* defect as positively charged when ESR active. As ESR signals do not provide any direct information about the charge state of the defect, then why this assignment? The evidence for this comes from another experiment, where ESR combined with capacitance-voltage ( $C$ - $V$ ) analysis has provided evidence for the *EX* defect being positively charged when ESR active.<sup>26</sup>

(2) The *EX* defect is modeled as a hole center, in line with the observation that  $g_{EX} > g_0 = 2.002319$ , the free-electron  $g$  value. It should be added, however, that the

property  $g > g_0$  of a defect's  $g$  value is generally not an exclusive criterion for hole center typification, as subtleties in the coupling scheme of the unpaired electron states may upset the general rule.

(3) The defect is an O-centric defect, with the unpaired electron not primarily localized at a Si site, which accounts for the absence of first-order  $^{29}\text{Si}$  hf interaction. Generally, a large hf splitting  $a \geq 400$  G would be expected<sup>1</sup> for an electron in an unpaired  $sp^3$  orbital centered at a single  $^{29}\text{Si}$  atom ( $I = \frac{1}{2}$ , 4.70% naturally abundant). For example, the prototype for such a defect orbital in  $\text{SiO}_2$  is the well-known class of intrinsic  $E'$  defects, incorporating various distinct species. All  $E'$  defects (except the unique  $E'_\delta$ , showing  $a \sim 100$  G, as expected for a four-way delocalized center) invariably show a strong  $^{29}\text{Si}$  hf doublet of splitting of  $\sim 410$  or 420 G, depending on whether it is measured in crystalline or glass surrounding.<sup>1</sup> No such strong  $^{29}\text{Si}$  hf structure could be traced in the *EX* spectrum, not even on thermally oxidized dispersed  $c$ -Si powder (average grain size  $\sim 5 \mu\text{m}$ ), where the *EX* signal's S/N ratio has been strongly enhanced.<sup>11</sup>

(4) The unpaired electron is postulated to be delocalized over four bordering O  $p$ -like orbitals. This may account for two results: First, an isotropic  $g$  value is possibly obtained through averaging out of the wave function's  $p$  character. Second, when following the model strictly, first-order  $^{17}\text{O}$  hf splitting will result from interaction with four O atoms, at more or less equivalent sites. With  $p(^{17}\text{O})=0.5122$ , this predicts a loss of central (unshifted) line intensity of  $\sim 87\%$  with respect to the  $^{17}\text{O}$  unenriched case, close to the experimental result of  $\sim 90\%$ . This picture is also corroborated by the simulation of the observed *EX*  $^{17}\text{O}$  hf structure (relative signal intensities), based on the standard LHO (localized hybrid orbital) description, concluding  $^{17}\text{O}$  hf interaction with  $\geq 4$  equivalent O atoms (see Sec. IV D). It is conceivable, however, that not all four central O atoms will occupy equivalent positions, due to structural relaxation that may have occurred. However, the resulting isotropy of the  $g$  factor would indicate their equivalence.

(5) The unpaired spin will undergo  $^{29}\text{Si}$  shf interaction with various Si sites. More precisely, along the strict model, the strongest  $^{29}\text{Si}$  shf structure likely<sup>27</sup> results from the first four equivalent neighboring Si sites, hence  $R \approx 0.2$  ( $R$  being the ratio of the hf intensity to the central line intensity). Although the experimental result would seem to indicate shf interaction with three equivalent Si sites (measured  $R \approx 0.14$ ), it is perhaps not unrealistic to keep open the feasibility for interaction with four Si sites: regardless of limited integration accuracies, the correct determination of  $R$  may be hampered by admixture of additional unresolved signals as well as unequal  $^{29}\text{Si}$  shf interaction over the various Si sites.<sup>5</sup> Consequently, regarding the  $^{29}\text{Si}$  shf, the model remains acceptable.

### C. Delocalized nature

The *EX* defect has been typified as a delocalized defect, i.e., the unpaired electron density extends over various

atomic orbitals with attendant smoothing of orbital anisotropy. This delocalization aspect may be looked at from two different perspectives.

Focusing the discussion on the outlined Si-vacancy model, one could, in a chemical bonding picture, envision the unpaired electron occupying a molecular orbital extending over all O atoms bordering the Si vacancy, viz. an extended molecular orbital (EMO) over a puckered O ring, a kind of a free radical. One consequence of this would be an approximately equally strong hf interaction with the four Si atoms in the first-neighbor Si shell—more or less as outlined in Ref. 28 for the  $V_{Si}^+$  model. If so, in its simplest case, it would also predict <sup>17</sup>O hf interaction with four equivalent O sites, with a hf splitting—to first order—about four times smaller than that of the single O-site situation, as is, e.g., the case for the NBOHC (i.e., the ≡Si—O· fragment). As outlined, this multiple equivalent-site character of the predicted hf interaction, both regarding <sup>17</sup>O and <sup>29</sup>Si, incorporates much of the attractiveness of the description.

At this point, however, it needs to be remarked that these assignments remain speculative, as they are based largely only on intensity ratio considerations, while the other crucial hf parameter, the hf splitting, has tacitly been left out. As already indicated, however, we may infer some indication of the expected hf interaction strength from other hf data for pertinent defects in *a*-SiO<sub>2</sub>. The NBOHC exhibits, for the isotropic part of the hf splittings, the values 26 and 14.4 G, for the <sup>17</sup>O hf and <sup>29</sup>Si shf structures, respectively.<sup>18,29</sup> When sticking to the idealized Si-vacancy model, implying shf interaction with four equivalent Si sites, one could thus expect, in a naive way, the values  $a(^{17}\text{O}) \approx 6.5$  G and  $a_{\text{shf}}(^{29}\text{Si}) \approx 4$  G. These should be compared with experimental results of  $\sim 14$  and 16.1 G, respectively. So if accepting the NBOHC defect as representative of the unpaired O bond in *a*-SiO<sub>2</sub>, the derived hf splittings for the Si vacancy model would appear somewhat small. However, it should be added that the exact appearance of the hf structure is dictated by the details of the unpaired electron's wave function, i.e., the spatial distribution over the various pertinent sites. So these hf splitting considerations may at present not suffice either to refute or approve the Si vacancy as the basic concept of EX.

Along a contrasting point of view, one could infer from the above analysis a warning that the Si-vacancy model—even if conceptually correct—is just not the exact statement of affairs, but rather only a working scheme that needs further refinement if not sincere revision.

A second approach could favor a more dynamic view. To set the picture, we start from an isolated Si vacancy, short of one electron, in an otherwise stoichiometric continuous SiO<sub>2</sub> network. This is schematically shown in Fig. 3(d), with the hole, in an initial configuration, localized on O atom *B*. This electronic structure, however, is clearly degenerate with respect to the configurations where the hole is respectively localized at the O sites *A*, *C*, and *D*. Nature may lift this symmetry (lowering the defect's energy state) through a spontaneous Jahn-Teller distortion (or, if a weak asymmetry is initially present, through a pseudo-Jahn-Teller distortion). This would im-

ply some (weak) atomic displacements leading to the formation of a (weak) bent O-O bond, as pictured in Fig. 3(e), leaving an ESR-active defect with one unpaired electron. This description, in effect, is in full analogy with the one first advanced in clear detail for the Si *E* center.<sup>30</sup>

Again, this situation is still degenerate both with respect to the bent bond formation and the unpaired electron's location—now with one additional aspect, however: Transitions from one configuration to another will face a (weak) potential barrier, embodying the previous Jahn-Teller distortion. However, coupling of the defect's electronic state to the network vibrational states will then lead to the so-called vibronic ground state, the result of this dynamic Jahn-Teller effect (DJT).<sup>31</sup> This may be pictured as a rapid hopping or tunneling of the unpaired electron among the various equivalent sites, attendant, of course, with the required O-O pair breaking and rebonding and structural deformation of the O cavity. This relaxation of the unpaired electron is described by a relaxation time  $\tau$ , which in a process characterized by an activation energy  $E_a$  may be expressed by an Arrhenius law  $\tau = \tau_0 \exp(E_a/kT)$ . The spin spends an average one-quarter of its time on each O atom bordering the Si vacancy, implying that, at any instant, the spin interacts with a primary O site and three first-neighbor O sites. In this picture, the Si vacancy is described as a dynamic entity, where an effectively isotropic, unpaired electron state results through averaging over four equivalent tetrahedral directions. If this hopping or tunneling occurs rapidly on the time scale of a Larmor period, the effective result regarding the delocalization of the unpaired electron, and hence the expected (s)hf interactions—both the <sup>17</sup>O hf and <sup>29</sup>Si shf interaction—will be *identical* to those for the EMO model. On the sensing time scale, the distinction between both descriptions fades. When applied to EX, it is evident that relaxation must be sufficiently rapid; that is,  $\tau$ , and hence  $E_a$ , must be accordingly small, as the remarkable isotropic state is still observed at temperatures as low as 4.3 K. In previous work, ESR observations have been extended down to 1.5 K, though without any sign of “quenching” of the defect spin in one particular configuration.<sup>32</sup>

#### D. Analysis of the experimental <sup>17</sup>O structure

As mentioned above, the advanced model pictures the EX spin as being delocalized over four equivalent O sites forming the cavity of a Si vacancy. The <sup>17</sup>O hf histogram for this EX model can readily be simulated (see, e.g., Refs. 12 and 33), if further assuming an *even* delocalization of the unpaired electron over the four O sites, hence described by a single hf matrix (apart, of course, from the unavoidable glass effect distortions). As outlined above, the effective hf structure appears isotropic, and is taken to be described by the isotropic splitting constant  $a$ . The result of the histogram calculation in this case is a 37-line spectrum, where the central line intensity now incorporates only a fraction  $I_c = 12.6\%$  of the initial intensity without <sup>17</sup>O hf splitting (see Fig. 4)—somewhat larger than the average of  $\sim 9.5\%$  observed experimentally.

To further test the current model, this calculation was

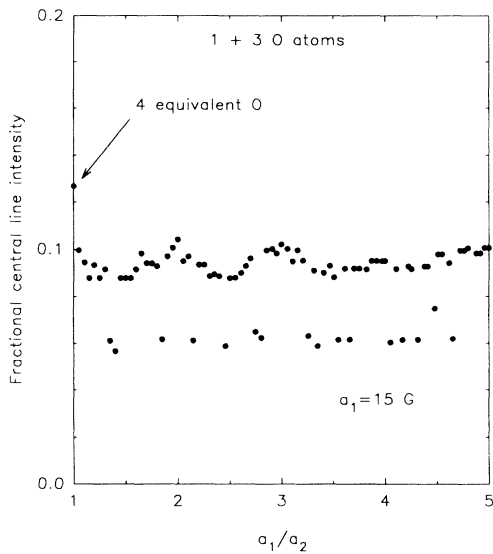


FIG. 4. Calculated fractional central line intensity of the  $EX$   $^{17}\text{O}$  hf structure within the framework of the Si-vacancy model for the  $EX$  defect as a function of the hf splitting ratio  $a_1/a_2$  (with  $a_1 = 15$  G) as explained in the text;  $a_1 = a_2$  corresponds to the case of four equivalent O sites.

also performed for the three, five, and six, equivalent O-sites cases, giving a central line intensity of 18%, 9.7%, and 8% of the initial intensity, respectively. When comparing with the experimental result, this would indicate that the  $EX$  spin interacts with five rather than four equivalent O sites. The next obvious step then is to analyze the equivalence of the various O sites with respect to the  $^{17}\text{O}$  hf interaction. There are hints<sup>28</sup> that, even within the Si-vacancy model, the four bonding O atoms do not relax equivalently, hence introducing variations in the hf interaction. Within the four O-site case, we have accordingly computationally reevaluated the central line intensity under the assumption that the defect spin is dynamically in stronger interaction (described by splitting  $a_1$ ) with one O site, and undergoes a weaker interaction (splitting  $a_2 \leq a_1$ ) with three equivalent O sites. As we have no measure of the hf splitting ratio  $a_1/a_2$ , we have included this number as a parameter which was varied starting from  $a_1/a_2 = 1$  (the previous case of four equivalent O sites) to larger values, corresponding to stronger interaction with one of the four O sites.

When working with two shells of equivalent O atoms, the determination of the  $EX$  central line intensity faces an extra problem: The use of two hf splitting constants drastically complicates the  $^{17}\text{O}$  histogram through manifold the number of component resonances ( $> 250$  for certain  $a_1/a_2$  values). This dictates that, when determining the relative central line intensity, one has to include lines in the histogram that are so close to the central line that, after convolution with the basic  $EX$  Voigt line shape to obtain the complete  $EX$   $^{17}\text{O}$  spectrum, they would be indistinguishable from the central resonance. As the  $EX$  central resonance has a derivative peak-to-peak width of  $\approx 1$  G,<sup>9</sup> the intensities of all histogram lines within a 1-G window centered at the central resonance are added to obtain the central line intensity as it

would be measured.

This quantification has implied to specify a value for  $a_1$ , which seems quite arbitrary at first sight and needs some explanation. In the case of four O sites treated equivalently ( $a_1/a_2 = 1$ ), the sextet of hf lines after the “first” splitting (interaction with one  $^{17}\text{O}$  nucleus) is clearly visible in the final histogram, these six lines having the largest intensity next to the central line. When varying then the ratio  $a_1/a_2$ , it was observed that this largely remains true for  $a_1/a_2 > 1$ : the six hf lines separated by  $a_1$  after the “first” splitting remain clearly distinguished in the final hf histogram. That is why the observed hf structure (see Fig. 2), especially lines  $h$ , is believed to belong to a first pair of these six rather well-resolved lines in the calculated histogram. As line  $h$  is  $\sim 7.5$  G from the  $EX_c$  line,  $a_1$  was first fixed at 15 G. Afterwards, however, having varied  $a_1$  around this value (10–20 G), it was shown that the calculated intensities are no function of the particular  $a_1$  value, thereby more or less validating our approach.

The central line fractional intensities  $I_c$  calculated as above are shown in Fig. 4 as a function of  $a_1/a_2$  with  $a_1$  fixed at 15 G. The arrow indicates the four equivalent O case ( $a_1 = a_2$ ), where  $I_c = 12.6\%$ . Once  $a_1/a_2 > 1$ , it is noticed that, while  $I_c$  remains generally within the 9–10% window, it may balance around 6–7% for some of the  $a_1/a_2$  values. The latter points in Fig. 4 are no artifact, but originate from the discrete nature of the histogram (lines moving in and out the 1-G window centered at the central line when  $a_1/a_2$  is changed<sup>34</sup>).

When reevaluating  $I_c$  as a function of  $a_1/a_2$  for the three and five O-site cases, it is found that this intensity varies between 12% and 15%, and 3% and 8%, respectively, making the hypothesis of four O sites somewhat more plausible. This would comply with the Si-vacancy picture.

It needs to be remarked that, since only a minor part of the presumed  $^{17}\text{O}$  hf structure could be resolved, the relative intensity ratio of the  $^{17}\text{O}$  hf structure to  $EX_c$  (though very pertinent) could not be included as a useful criterion in this evaluation. We thus may infer two main conclusions from the  $^{17}\text{O}$  hf structure computer simulations. First, regarding the observed relative central-line intensity and observed hf splitting, the experimental results may well be accounted for by interaction of the unpaired electron with four O sites. Second, *not all* four O sites appear *equivalent*. The most satisfactory result is obtained for interactions with one O site in a first shell and three O sites in a second shell (in agreement with the  $V_{\text{Si}}^+$  model<sup>28</sup>). The observed  $^{17}\text{O}$  hf structure may thus be reconciled with the basic Si-vacancy picture.

In a last remark, we would like to point out that detailed analysis of the  $EX$   $^{29}\text{Si}$  shf structure will likely require the incorporation of the same principle; that is, treating the various Si sites slightly inequivalently. However, the effect will be smaller as the Si atoms are located at first-neighbor sites.

#### E. Viability of the Si-vacancy model

While we are unaware of any previous experimental ESR report of the undecorated Si vacancy  $V_{\text{Si}}$  in  $\text{SiO}_2$ ,

there has been some theoretical work. Using the self-consistent semiempirical quantum-chemical method MINDO/3 (modified intermediate neglect of differential overlap<sup>35</sup>), Dianov, Sokolov, and Sulimov<sup>28</sup> calculated the electronic properties of the Si vacancy centered at a H-terminated stoichiometric vitreous SiO<sub>2</sub> cluster of minimal size. Five charge states of the defect were considered, i.e.,  $V_{\text{Si}}^{2-}$ ,  $V_{\text{Si}}^{-}$ ,  $V_{\text{Si}}^0$ ,  $V_{\text{Si}}^{+}$ , and  $V_{\text{Si}}^{2+}$ , where allowance has been made for structural relaxation of the vacancy-bordering O atoms. For the  $V_{\text{Si}}^{+}$  case, i.e., basically the EX model depicted in Fig. 3(f), they find the core of this defect to consist of four  $\equiv\text{Si}-\text{O}\cdot$  entities where no bonds between the O atoms occur. These entities, however, are closely spaced, and hence strongly interacting, with the unpaired electron mainly localized on four O sites, three of them behaving as approximately equivalent sites. But while there appears some qualitative agreement with the salient EX ESR results, the  $V_{\text{Si}}$  theory fails quantitatively. For one, it predicts an axial g matrix with  $g_{\perp} \approx 1.998$  and  $g_{\parallel} \approx 2.002$ , in contrast with the EX result. However, a main concern is that the  $V_{\text{Si}}$  model predicts that the formation of  $V_{\text{Si}}^{+}$  by trapping a hole at  $V_{\text{Si}}^0$  would cost  $18.2 - 5.4 = 12.8$  eV; as the uppermost oxygen orbitals housing the unpaired spin in this O-cluster model are likely close in energy to the SiO<sub>2</sub> valence band, that value seems unrealistically high, thus undermining the confidence in the calculations.

There is one general remark regarding theoretical modeling. It deals with the notion that the Si vacancy likely emerges as a result of strongly *nonequilibrium* processes. Such property may appear a conceivable aspect of the EX center when referring to the particular circumstances of EX generation; that is, transformation of *c*-Si into an *a*-SiO<sub>2</sub> network layer by layer through violent oxidation reactions under an abundance of O<sub>2</sub>. In effect, the EX defects generated during thermal oxidation are seen as the incarnation of a nonequilibrium process. Here, a necessary distinction between a *damage* defect, introduced by some energetic particle in a continuous atomic structure, and a *natural* defect, introduced during network growth, comes to the fore. In terms of the Si vacancy in *a*-SiO<sub>2</sub>, we should distinguish between a Si atom kicked out of its regular network position by, e.g., a  $\gamma$  photon—thus creating a Si vacancy in an otherwise continuous *a*-SiO<sub>2</sub> network—and a grown-in Si vacancy, which, in one picture, may be seen as the mismatch result at the meeting borders of different, independently formed, oxide granulates: the damage defect may be generated in an initially continuous network, while, in the natural defect case, network discontinuity may be the natural result from growth constraints. It seems not unreasonable to expect that the difference between these two extreme formation circumstances will reflect in unequal arrangements (structural relaxation) of the immediate Si-vacancy surrounding. This may prove to be an obstacle for successful theoretical analysis.

Various effects may be at the heart of the nonequilibrium aspect; besides the above-mentioned geometrical constraint effect, one could instead refer to a possible influence of water, or more generally  $-\text{OH}$  termination, that might impair the growth of a continuous *v*-SiO<sub>2</sub> net-

work, through obstructive bond termination. A hint into that direction may come from the OHC defect formation, which is seen predominantly as a result of the radiolysis of an abundance of  $\equiv\text{Si}-\text{OH}$  precursor sites in *v*-SiO<sub>2</sub>.<sup>1</sup>

#### F. Association with other defects

In characterizing the EX defect, it might be useful to investigate any possible relationship of the EX center, as sensed through its ESR properties, with the defects previously identified by ESR in SiO<sub>2</sub> either in crystalline or vitreous states.

Restricting ourselves to the group of intrinsic defects, two classes of defects may be distinguished, i.e., Si-centric and O-centric defects, reflecting the chemical composition of SiO<sub>2</sub>. The first class includes the widely studied  $E'$  family, also referred to as O-vacancy defects, with the  $\equiv\text{Si}\cdot$  fragment as common defect entity. It is clear that the present result, delineating EX as an O-centric defect, rules out any relationship of EX with the various  $E'$  type defects, except perhaps the  $E'_8$  variant, for which no conclusive atomic model yet exists. Like the EX center, the latter is also interpreted as a delocalized defect, its factual relationship with the traditional  $E'$  centers still being unclear.

The second, O-centric class, includes the NBOHC, the peroxy radical (PR), and the most recently described self-trapped holes (STH's),<sup>36</sup> all exhibiting distinct anisotropy. Hence the relationship of the EX defect with a *solitary* species of any of these types seems to be excluded on the ground of the EX defect's highly isotropic g matrix. As mentioned above, this exclusion does not apply to intimate combinations of such defects, resulting in electronically strongly modified defect centers. In fact, such a multiple O-centric agglomerate is suggested as the embryo of the EX defect.

Finally, as the EX center concerns a recent observation, we may try to correlate it with defects expected or predicted to occur—though not yet observed by ESR—in SiO<sub>2</sub>, or, more specifically, in the thermal Si/SiO<sub>2</sub> entity. In this connection, one may try to correlate the EX defect with a single moiety of a valence-alternation pair (VAP) proposed to exist in SiO<sub>2</sub>.<sup>37</sup> In its simplest description, such a VAP is supposed to involve an oppositely charged nearby pair of overcoordinated and undercoordinated oxygen atoms, symbolized in the SiO<sub>2</sub> case as  $\text{O}_1^-$  and  $\text{O}_3^+$ ; the  $\text{O}_3^+$  entity, with the O atom attached to three Si atoms, is also referred to as oxonium. However, when in their neutral charge state—as required to be ESR active— $\text{O}_1^0$  and  $\text{O}_3^0$  would become NBOHC and  $E'$ -like centers, respectively, in clear conflict with the EX properties; their monoatomic O or Si-centric defect kernel is inappropriate.

#### V. SUMMARY

The <sup>17</sup>O structure of the EX defect in thermal SiO<sub>2</sub> has been resolved through <sup>17</sup>O enrichment. Although only part of the <sup>17</sup>O structure could be observed, it has unveiled basic information regarding the defect's atomic nature. First, the impact of the <sup>17</sup>O enrichment, in com-

bination with relative spectral line intensity considerations, definitely categorizes *EX* as an oxygen-centric defect. Second, it is found to possess a multiple oxygen kernel, the unpaired electron being delocalized over four O sites which may be slightly inequivalent.

This, in combination with a previously identified  $^{29}\text{Si}$  hf structure, points in the direction of a simple Si vacancy as the most elementary working model; the unpaired electron would thus exhibit a  $^{29}\text{Si}$  shf interaction with four neighboring Si sites. The magnitude of the respective hf splittings, though comparable, comes out somewhat larger than the values qualitatively derived from the measured properties of the unpaired  $2p$  O electron of the NBOHC—an effect that may likely be accounted for by the details of the delocalized nature of the unpaired spin.

As a final remark, we would like to emphasize that although the Si-vacancy model may well serve as the “best choice” working scheme, it is not considered as finally proved or correct in every detail. It is, however, con-

sidered a suitable platform from which improvements may be implemented. Theoretical analysis, in combination with improved hf data—including the detection of both the full  $^{17}\text{O}$  and  $^{29}\text{Si}$  hf structure—may be worth the effort as the *EX* defect seems so far to be the sole intrinsic natural defect detected by ESR in  $\alpha\text{-SiO}_2$ . Unveiling the defect’s exact structure may enhance our understanding of fundamental properties as well as the growth kinetics of thermal  $\text{SiO}_2$ . Its natural presence in the basic Si/ $\text{SiO}_2$  entity may adduce another motive for its fundamental analysis.

#### ACKNOWLEDGMENTS

The authors are grateful for helpful and encouraging discussions with David Griscom. Support to this work by the Belgian National Fund for Scientific Research is gratefully acknowledged.

- 
- <sup>1</sup>D. L. Griscom, in *Glass Science and Technology*, edited by N. J. Kreidl and D. Uhlman (Plenum, New York, 1990), Vol. 4B, p. 151.
- <sup>2</sup>Y. Nishi, *Jpn. J. Appl. Phys.* **10**, 52 (1971).
- <sup>3</sup>E. H. Poindexter and P. J. Caplan, *Prog. Surf. Sci.* **14**, 211 (1983).
- <sup>4</sup>P. J. Caplan, E. H. Poindexter, B. E. Deal, and R. R. Razouk, *J. Appl. Phys.* **50**, 5847 (1979); E. H. Poindexter, P. J. Caplan, B. E. Deal, and R. R. Razouk, *ibid.* **52**, 879 (1981).
- <sup>5</sup>K. L. Brower, *Appl. Phys. Lett.* **43**, 1111 (1983).
- <sup>6</sup>A. Stesmans, *Appl. Phys. Lett.* **48**, 972 (1986).
- <sup>7</sup>A. H. Edwards, *Phys. Rev. B* **36**, 9638 (1987).
- <sup>8</sup>M. Cook and C. T. White, *Phys. Rev. Lett.* **59**, 1741 (1987).
- <sup>9</sup>A. Stesmans, *Phys. Rev. B* **45**, 9501 (1992); *Solid State Commun.* **82**, 809 (1992).
- <sup>10</sup>A. Stesmans, *Phys. Rev. B* **48**, 2418 (1993).
- <sup>11</sup>A. Stesmans and F. Scheerlinck, *J. Appl. Phys.* **75**, 1047 (1994).
- <sup>12</sup>G. Van Gorp and A. Stesmans, *Phys. Rev. B* **45**, 4344 (1992); G. Van Gorp, Ph.D. thesis, Katholieke Universiteit Leuven, 1991.
- <sup>13</sup>A. Stesmans, *J. Magn. Res.* **76**, 14 (1988).
- <sup>14</sup>(111)Si samples are preferred for this work for reasons of minimal  $P_b$  interface defect interference with the *EX* signal. Choosing  $\text{B}\parallel(111)$  ensures that the anisotropic  $P_b$  signal is shifted farthest away ( $g \approx 2.0086$ ) from the central *EX* signal ( $g \approx 2.0025$ ).
- <sup>15</sup>G. Feher, *Phys. Rev.* **114**, 1219 (1959).
- <sup>16</sup>A. Stesmans and J. Braet, *Surf. Sci.* **172**, 398 (1986).
- <sup>17</sup>A. Stesmans and Y. Wu, *Solid State Commun.* **62**, 435 (1987).
- <sup>18</sup>M. Stapelbroek, D. L. Griscom, E. J. Friebele, and G. H. Sigel, Jr., *J. Non-Cryst. Solids* **32**, 313 (1979).
- <sup>19</sup>See, e.g., D. L. Griscom, *Rev. Solid State Sci.* **4**, 565 (1990).
- <sup>20</sup>D. L. Griscom, *Phys. Rev. B* **22**, 4192 (1980).
- <sup>21</sup>We refrain from including the sign of  $a$  in this discussion as we have no information on this from our  $^{17}\text{O}$  hf observations.
- <sup>22</sup>D. L. Griscom and E. J. Friebele, *Phys. Rev. B* **34**, 7524 (1986).
- <sup>23</sup>D. L. Griscom, *Nucl. Instrum. Methods Phys. Res. B* **1**, 481 (1984).
- <sup>24</sup>K. Vanheusden and A. Stesmans, *Appl. Phys. Lett.* **62**, 2405 (1993); *J. Appl. Phys.* **74**, 275 (1993).
- <sup>25</sup>R. H. D. Nuttall and J. A. Weil, *Solid State Commun.* **33**, 99 (1980).
- <sup>26</sup>A. Stesmans and F. Scheerlinck, *Appl. Phys. Lett.* **64**, 2282 (1994).
- <sup>27</sup>It is well known that core polarization effects on the unpaired-spin density away from the defect core may turn over the shf interaction strength naively expected if the spin were extending into a uniform continuum (Ref. 8).
- <sup>28</sup>E. M. Dianov, V. O. Sokolov, and V. B. Sulimov, *Phys. Status Solidi B* **160**, 262 (1990).
- <sup>29</sup>D. L. Griscom and E. J. Friebele, *Phys. Rev. B* **24**, 4896 (1981).
- <sup>30</sup>G. D. Watkins and J. W. Corbett, *Phys. Rev.* **134A**, 1359 (1964).
- <sup>31</sup>F. S. Ham, *Phys. Rev.* **166**, 307 (1968).
- <sup>32</sup>A. Stesmans and F. Scheerlinck, *Microelectron. Eng.* **22**, 139 (1993).
- <sup>33</sup>G. E. Pake and T. L. Estle, *The Physical Principles of Electron Paramagnetic Resonance* (Benjamin, London, 1973).
- <sup>34</sup>When the resolution in Fig. 4 is increased (smaller steps when varying  $a_1/a_2$ ), it is observed that both “bands” become more explicit.
- <sup>35</sup>See, e.g., A. H. Edwards and W. B. Fowler, *J. Phys. Chem. Solids* **46**, 841 (1985).
- <sup>36</sup>D. L. Griscom, *J. Non-Cryst. Solids* **149**, 137 (1992).
- <sup>37</sup>G. Lucovsky, *J. Phys. Soc. Jpn.* **49**, 1129 (1980); K. C. Snyder and W. B. Fowler (unpublished); G. M. Greaves, *J. Non-Cryst. Solids* **32**, 295 (1979).